Journal of the European Ceramic Society 37 (2017) 3425–3434

Contents lists available at www.sciencedirect.com

Journal of the European Ceramic Society

journal homepage: www.elsevier.com/locate/jeurceramsoc

Preparation of nanostructured $Gd_2Zr_2O_7$-$LaPO_4$ thermal barrier coatings and their calcium-magnesium-alumina-silicate (CMAS) resistance

Mingzhu Li[a,b,c], Yuxian Cheng[d], Lei Guo[a,b,c,*], Yuchen Zhang[a,b], Chenglong Zhang[a,b,c], Sixian He[a,b], Wei Sun[a], Fuxing Ye[a,b,c]

[a] School of Materials Science and Engineering, Tianjin University, China
[b] Tianjin Key Laboratory of Advanced Joining Technology, Tianjin University, China
[c] Key Lab of Advanced Ceramics and Machining Technology of Ministry of Education, Tianjin University, No. 92, Weijin Road, Tianjin 300072, China
[d] AECC Shenyang Liming Aero Engine Group Corporation Ltd., Shenyang 110043, China

ARTICLE INFO

Article history:
Received 25 November 2016
Received in revised form 28 February 2017
Accepted 29 March 2017
Available online 5 April 2017

Keywords:
Thermal barrier coatings (TBCs)
Doped $Gd_2Zr_2O_7$
Air plasma spraying (APS)
Nanostructure
Calcium-magnesium-alumina-silicate (CMAS)

ABSTRACT

Nanostructured 30 mol% $LaPO_4$ doped $Gd_2Zr_2O_7$ ($Gd_2Zr_2O_7$-$LaPO_4$) thermal barrier coatings (TBCs) were produced by air plasma spraying (APS). The coatings consist of $Gd_2Zr_2O_7$ and $LaPO_4$ phases, with desirable chemical composition and obvious nanozones embedded in the coating microstructure. Calcium-magnesium-alumina- silicate (CMAS) corrosion tests were carried out at 1250 °C for 1–8 h to study the corrosion resistance of the coatings. Results indicated that the nanostructured $Gd_2Zr_2O_7$-$LaPO_4$ TBCs reveals high resistance to penetration by the CMAS melt. During corrosion tests, an impervious crystalline reaction layer consisting of Gd-La-P apatite, anorthite, spinel and tetragonal ZrO_2 phases forms on the coating surfaces. The layer is stable at high temperatures and has significant effect on preventing further infiltration of the molten CMAS into the coatings. Furthermore, the porous nanozones could gather the penetrated molten CMAS like as an absorbent, which benefits the CMAS resistance of the coatings.

1. Introduction

Thermal barrier coatings (TBCs) serve as the first line of defense in the hot-section metallic components of gas-turbine engines [1–5]. They have many desirable attributes such as low thermal conductivity, good high-temperature capability and high compliance, which impart them with positive function on improving the performance and efficiency of the engines. The successfully and widely used TBCs are made of yttria partially stabilized zirconia (YSZ). Various techniques have been explored to fabricate TBCs, including air plasma spraying (APS), electron beam physical vapor deposition (EB-PVD), and plasma spray physical vapor deposition (PS-PVD) [5–9]. By the use of the TBCs, the maximum operating temperature of gas-turbine engine has been increasing steadily. However, higher operating temperature makes TBCs more susceptible to environmental deposits damage [10–14]. During engine operation, fly ash, sand, volcanic ash and runway debris are ingested with the intake air. When the coating surface is as hot as 1200 °C, these deposits melt and penetrate into the coating causing it to spall-off. The environmental deposits are commonly referred to as calcium-magnesium-alumina-silicate (CMAS). Recently, CMAS attack is becoming a great challenge for the further development of TBCs. Thus, there is a great need to develop protective measurements for TBCs against damage from CMAS.

The degradation mechanisms by which molten CMAS attacks YSZ TBCs have been documented in open literature [7,13,15–20]. Molten CMAS has low viscosity and excellent wetting characteristics, which impart it with strong ability to penetrate into pores/cracks in the TBCs. As a result, tetragonal YSZ grains dissolve in the melt. The Zr^{4+} saturation of the melt induces the precipitation of tetragonal Y_2O_3 depleted ZrO_2. Upon cooling, the tetragonal Y lean-ZrO_2 experiences a phase transformation to monoclinic ZrO_2, associated with a 3–5% volume expansion which could lead to cracks in the coating [1,7,17]. Additionally, the CMAS-impregnated TBCs reveal low strain-tolerance, which make them highly vulnerable to thermo-mechanical failure during thermal cycling [18–21].

Extensive efforts have been devoted to developing CMAS protection methods for TBCs. Some researchers have suggested depositing a de-wetting outer layer or introducing a sacrificial layer on the top

* Corresponding author at: School of Materials Science and Engineering, Tianjin University, China.
E-mail addresses: glei028@tju.edu.cn, glei028@163.com (L. Guo).

http://dx.doi.org/10.1016/j.jeurceramsoc.2017.03.069
0955-2219/

surface of the TBCs [22–24]. The rationale behind these approach is to reduce the amount of CMAS deposits on the coating or to arrest the propagating CMAS front. However, limited success seems to be obtained, which mainly be attributed to the large thermal expansion mismatch between the introduced layers and the TBCs. Krämer et al. first indicated that $Gd_2Zr_2O_7$ has high resistance to CMAS attack [25]. Dissolution of $Gd_2Zr_2O_7$ into the CMAS leads to the rapid formation of an apatite silicate phase $Ca_2Gd_8(SiO_4)_6O_2$ and a $Zr(Gd,Ca)O_x$ fluorite phase. The combination of these two phases forms a layer which arrests CMAS infiltration. Then, investigation revealed that the poor resistance of YSZ TBCs to CMAS attack is due to their low Y_2O_3 content [15,26]. Padture et al. increased the Y^{3+} content in YSZ TBCs, and found that the CMAS penetration is effectively arrested mainly attributed to the precipitation of apatite phase [27,28].

Besides $Gd_2Zr_2O_7$, other TBC candidates, such as $La_2Zr_2O_7$, $La_2Ce_2O_7$, $La_2(Zr_{0.7}Ce_{0.3})_2O_7$ and $LaMgAl_{11}O_{19}$, have also been found to exhibit excellent CMAS resistance [29–32]. The rationale behind these desirable attributes is similar, attributable to the precipitation of apatite phase and other compounds with high melt temperature, leading to the formation of a sealing layer on the coating surface. Among many TBC candidates, $Gd_2Zr_2O_7$ has attracted great attention due to its excellent phase stability, desirable thermo-physical properties and good CMAS resistance characteristic [15,33]. $Gd_2Zr_2O_7$ TBC has been successfully fabricated and thermal cycling tests with coating surface temperature above 1300 °C indicated that it has superior high temperature capability and thermal insulation compared with YSZ TBCs. However, the thermal cycling lifetime of $Gd_2Zr_2O_7$ TBC is still unsatisfactory, mainly attributable to its poor toughness [34–36]. Our previous research has found that $LaPO_4$ could be designed as a toughening agent for $Gd_2Zr_2O_7$, and the optimal $LaPO_4$ addition content is around 30 mol% [37].

Recently, nanostructured TBCs produced by APS have attracted particular attention due to their superior performance compared with their conventional counterparts [38–41]. Notice that the "nanostructured coating" is a coating containing nanozones embedded in the coating microstructure, rather than completely consisting of nano particles. The nanozones impart the coatings with high interlamellar strength, excellent crack propagation resistance, good thermal insulation and desirable molten salt corrosion resistance [38,39]. However, in spite of the importance of the nanostructured coatings, their preparation is challenge, especially for producing the coatings with novel materials. In our previous study, we have indicated that 30 mol% $LaPO_4$ doped $Gd_2Zr_2O_7$ ($Gd_2Zr_2O_7$-$LaPO_4$) is a promising TBC candidate material [37]. However, there is limited report on the fabrication of $Gd_2Zr_2O_7$-$LaPO_4$ coatings, especially for the coatings with nanostructure. In this study, attempt is carried out to produce nanostructured $Gd_2Zr_2O_7$-$LaPO_4$ TBCs by APS. The coatings are then exposed to molten CMAS at 1250 °C for 1 h, 4 h and 8 h. The CMAS resistance characteristics of the coatings are evaluated and the related mechanisms are discussed.

2. Experimental procedure

$Gd_2Zr_2O_7$ and $LaPO_4$ nano powders were both fabricated by a chemical coprecipitation and calcination method, and the detailed preparation procedures were described elsewhere [33,37]. Subsequently, $Gd_2Zr_2O_7$ and 30 mol% $LaPO_4$ powders were mixed by ball milling for 8 h at a speed of 400 rpm, followed by drying at 120 °C for 8 h and calcination at 1000 °C for 5 h for crystallization. A spray drying method was used to produce $Gd_2Zr_2O_7$-$LaPO_4$ microscopic particles for thermal spray. Stainless steel was used as substrate, on which the coating was directly deposited by an APS facility (APS-2000, China). The operating parameters selected from the pre-optimization procedures are listed in Table 1. After the deposition, the substrate was mechanically removed to obtain free-standing ceramic coatings.

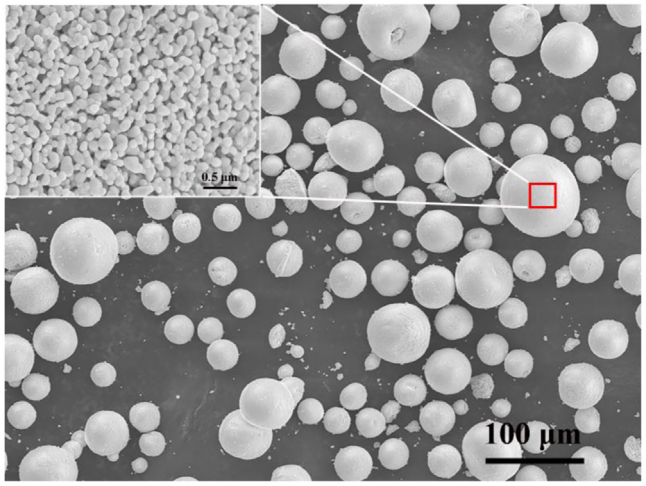

Fig. 1. SEM micrograph of $Gd_2Zr_2O_7$-$LaPO_4$ agglomerated particles. The inset image reveals detailed morphology of individual particle.

CMAS with a composition of 22CaO-19MgO-14$AlO_{1.5}$-45SiO_2 in mole ratio was used in this study. It was determined based on the literature [7,30] and reflected the average composition of deposits on vane blades in aircraft engines operated in China. The raw materials were carefully weighted in the molar ratio and suspended in deionized water. Then, they were mixed via planetary ball milling for 5 h at a speed of 400 rpm, followed by drying at 120 °C for 6 h. The obtained CMAS powders were dispersed in absolute alcohol and fully stirred to produce homogeneous suspension. The resultant suspension was dropped on the surfaces of $Gd_2Zr_2O_7$-$LaPO_4$ coatings with a concentration of about 20 mg/cm^2. After the evaporation of the alcohol, the coating surface was evenly covered with CMAS deposits. Then, the samples were heat-treated in box electric furnace (SX-1600 °C) at 1250 °C for 1 h, 4 h and 8 h.

Phase composition was characterized by an X-ray diffraction (XRD, Bruker D8 Advanced, Germany) using Cu Kα radiation. Data were digitally recorded in a continuous scan in 2θ range of 10°–90° with a scanning rate of 0.1°/s. Raman spectra were recorded by a microscopic confocal Raman spectrometer (RM2000; Renishaw, Gloucestershire, UK) using 514.5 nm excitation from an argon ion laser. The spectral resolution was about 1 cm^{-1}. The Raman spectrum was collected at a rate of 600 cm^{-1}/30 s and accumulated by triple scanning. Surface morphologies and composition analysis were carried out by a scanning electron microscope (SEM; TDCLS4800, Hitachi Ltd., Japan) equipped with energy dispersive spectroscopy (EDS, IE 350), and cross-sectional images were taken by a scanning electron microscope (SEM; TDCLSU1510, Hitachi Ltd., Japan). Transmission electron microscopy (TEM) specimens from the coating after 1 h CMAS corrosion were prepared using a focused ion beam (FIB) and the morphologies were observed by a transmission electron microscope (TEM, JEM-2100, Japan) equipped with energy dispersive spectrum (EDS).

3. Results and discussion

Fig. 1 shows the SEM image of $Gd_2Zr_2O_7$-$LaPO_4$ agglomerated particles. All the particles reveal spherical shape, with a size distribution ranging from 10 to 50 μm. The inset image reveals that the microscopic particle has porous structure and consists of many nanosized particles, i.e. smaller than 100 nm. EDS result in Table 2